Complexes of C60 with Cyclic Oligothiophenes: A Theoretical Study

Manuel Garcia, Patricia Guadarrama, and Serguei Fomine*

Instituto de Investigaciones en Materiales, Universidad Nacional Autónoma de México, Apartado Postal 70-360, CU, Coyoacán, Mexico DF 04510, México

Received: January 25, 2010; Revised Manuscript Received: March 23, 2010

Complexes of C60 and cyclic and linear oligothiophenes containing 8 and 12 repeating units have been modeled at the M05-2X/6-311G**//M05-2X/6-31G* level of theory. BSSE-corrected binding energies of neutral donor−acceptor complexes vary from 5 to 12 kcal/mol depending on the complex and donor type. Inclusion complexes formed by C60 and cyclooligothiophenes containing 8 repeating units were found to be the most stable ones. Only weak charge transfer from oligothiophene to C60 fragment (<0.1 electron) is observed in the ground state, whereas complete electron transfer from oligothiophene fragment to C60 has been found in the excited state. One electron oxidation or reduction increases binding energies of "tight" complexes and decreases donor−acceptor interaction for "loose" complexes. In the case of cation radicals, positive charge is totally concentrated at the oligothiophene fragment, whereas in anion radicals, negative charge is located at the C60 moiety. Calculations demonstrated that plane oligothiophene conformation and weak binding in a donor−acceptor complex favor the photoinduced charge-carrier formation.

Introduction

The actual trend in research and development of novel photovoltaic materials is intended to discover a credible cost/efficiency compromise to make feasible their use as power sources. The polymer-based organic photovoltaic devices have introduced the possibility of developing cheap and easy techniques to generate energy from light.[1] In 1986, Tang[1b] accomplished a 1% power conversion efficiency with an organic photovoltaic cell based on low-molecular-weight organic thin film, and since then great advances have been made resulting in a numerous strategies to improve the performance of solar cells based on polymers.[2] Solar cells based on conjugated polymers alone have been promising candidates for use in low-cost electronics and photovoltaic devices;[3] however, their quantum efficiency was low. Nonetheless, mixing electron-donor-type polymers with suitable electron acceptors[4] resulted in highly efficient materials because of effective breaking apart of excitons into free charge carriers. Among electron-donor-type polymers, polythiophenes probably are the most important materials for photovoltaic devices because of their excellent performance and power conversion efficiencies.[5] Presently, the highest power conversion efficiency for single polymers and fullerene derivatives[6] achieved 7.4%. It has also been demonstrated that molecular architecture of polythiophene has important consequences on the electronic properties, as has been shown for 2D macrocyclic,[7] disk- and starlike,[8] as well as for 3D cruciform,[9] catenated,[10] and branched dendritic[11] oligothiophenes. Theoretical calculations have also demonstrated that 2D macrocyclic oligothiophenes are able to form stable tubular aggregates because of $\pi-\pi$ stacking between macrocycles.[12] Moreover, it has recently been demonstrated[13] that 2D macrocyclic oligothiophenes are able to form complexes with C60. C60-fullerenes are adsorbed in a monolayer of cyclo[12] thiophene and self-assemble in a second layer whose crystallinity is governed by the formation of 1:1 π-donor−π-acceptor (**D-A**) complexes. Two different types of complexes were detected:

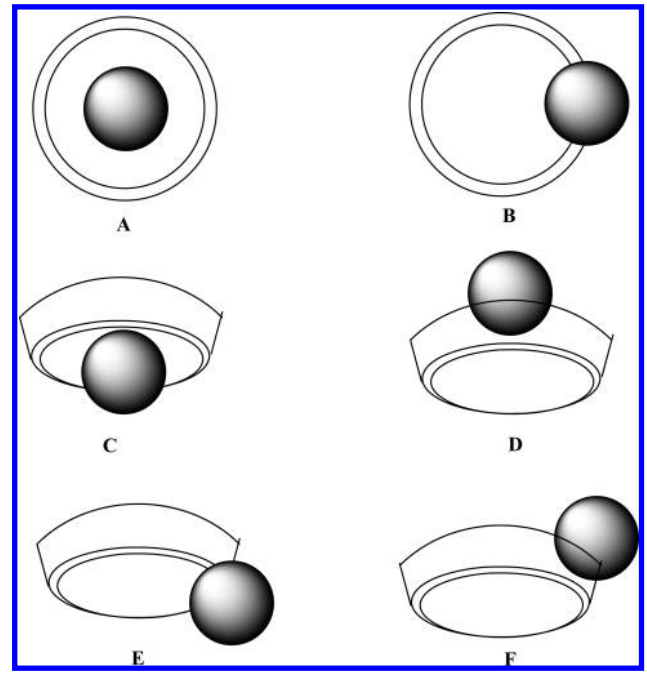

Figure 1. Mutual orientation of C60 and cyclooligothiophene in C60−cyclooligothiophene complexes. Apart from **A** and **B** complexes, **C**, **D**, **E**, and **F** configurations are also possible for substituted cyclooligothiophenes.

type **A**, where C60 is located in the internal cavity of a macrocycle, and type **B**, where C60 is placed at the rim of macrocycle (Figure 1). Experimental data suggested that the complex of **B** type is the most stable for cyclooligothiophene containing 12 repeating units. Because complexes of fullerenes with cyclic oligothiophenes could be possible candidates for applications in photovoltaic devices, the aim of this manuscript is to obtain deeper insight into the electronic structure of these complexes to describe the nature of the donor/acceptor interface that plays a determinant role in the magnitude of the open-circuit voltage directly proportional to the power conversion efficiency

* Corresponding author.

10.1021/jp1007347
Published on Web 04/05/2010

of a solar cell.[14] The effect of the molecular architecture will also be addressed, analyzing the differences between linear and cyclic oligothiophenes as donor moieties of these complexes.

Computational Details

The modeling of charge transfer (CT) complexes, where dispersion interactions have an important contribution to the total binding energy, is a challenging task requiring methods taking into account dynamic correlation. It has been previously shown[12] that the MPWB1K functional performs well for $\pi-\pi$ stacking interaction in complexes of cyclic oligothiophenes. In this work, however, we applied M05-2X functional combined with the 6-31G(d) basis set for geometry optimizations, followed by a single-point energy calculations using the larger 6-311G(d,p) basis set. Restricted and unrestricted formalisms were used for closed shell (neutral) and open shell systems (cation and anion radicals), respectively. No counterions were considered for charged molecules.

The M05-2X functional belongs to the fourth rung of Jacob's ladder,[15] incorporating electron spin density, density gradient, kinetic energy density, and Hartree−Fock (HF) exchange. This particular functional incorporates 56% of HF exchange. Calculations were carried out using the Gaussian 09[18] suit of programs. Basis set superposition errors (BSSE) have been estimated for all complexes using the counterpoise correction method implemented in Gaussian 09 code. In its original form, DFT is applicable only to ground states. The Runge−Gross theorem[19] extends the theory into the time domain, called time-dependent DFT (TD-DFT), thus allowing the treatment of electronically excited states. Currently, TD-DFT is the most widely applied tool for modeling electronic spectra.[20]

M05-2X overperforms MPWB1K functional for $\pi-\pi$ stacking energies;[15] moreover, the time-dependent M05-2X (TD-M05-2X) model reproduces excitation energies of cyclic oligothiophenes and a model CT complex between aniline and *o*-chloranile within 0.2 eV.[16]

In addition, the M05-2X model reproduces within 0.1 eV the LUMO energy of C60 measured in acetonitrile (3.7 and 3.8 eV (exp)[17]). Therefore, the M05-2X functional provides a reliable description of the systems under investigation.

Synthesized cyclooligothiophenes have *n*-butyl side groups.[13] *n*-Butyl groups have been replaced by methyl groups in the studied model complexes. Complexes formed by unsubstituted cyclooligothiophenes and their linear analogues were studied as well for the comparison purposes. According to experimental data, alkyl substituents are situated only on the one side of a macrocycle adopting a "spider-like" conformation, and this conformation has been selected as starting geometry for the optimizations. Cyclooligothiophenes containing 8 and 12 repeating units as donor fragments for the complex formation are shown in Figure 2. Results of linear oligothiophenes are denoted **Ln**, and those for the complexes between C60 and a linear thiophene molecule are indicated as **LCn**, where n is the number of repeating units in linear oligothiophene. Cation and anion radicals are referred to as + and −, respectively.

To model the donor−acceptor interface of a solar cell (Figure 7), the calculations for donor components were carried out using the PCM solvation model implemented in Gaussian 09 using a dielectric constant of 4.0 (polythiophene)[21] and the rest of the parameters as defined for thiophene. Dielectric constant of 4.0 was used for C60[22] and the solvent radius of 5 Å (external radius of C60). To describe CT complexes at the donor−acceptor interface, dielectric constant of 4.0 and solvent radius of 3.76 Å were used (mean value between thiophene and C60).

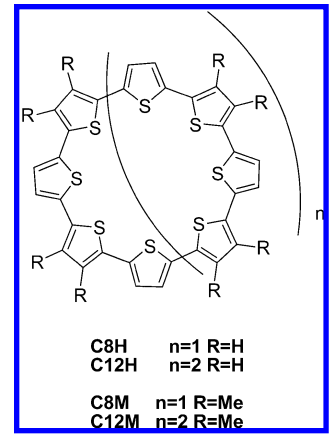

Figure 2. Cyclooligothiophene host molecules.

Results and Discussion

Geometry of C60−Cyclooligothiophene Complexes. Figure 3 depicts the geometries of optimized complexes. In the case of cyclooligothiophenes **C8H** and **C8M**, the only detected complex is that where fullerene C60 interacts with the cavity of a cyclooligothiophene (complexes **C8HA** and **C8MD**). As seen from Figure 3, the complex formation between cyclooligothiophenes containing eight repeating units and C60 results in a drastic change in the macrocycle conformation. Therefore, the lowest energy conformation of **C8H** is D_{4d}, whereas in **C8HA**, the macrocycle adopts a conic (C_{4v}) conformation (Figure 3) to maximize the overlap between π orbitals of C60 and the corresponding orbitals of oligocyclothiophene macrocycle. Similar situation can also be observed for the complex **C8MD**.

In this sense, the behavior of **C8H** and **C8M** in C60 complexes differs from that observed for tubular complexes of **C8H**, where a tubular structure of macrocycles united by $\pi-\pi$ interactions is formed without significant conformation changes.[12a] Unlike **C8H** and **C8M**, **C12H** and **C12M** form a variety of different complexes with C60. **C12H** forms two different types of complexes **A** and **B**, whereas for methyl-substituted **C12M**, at least five different configurations are possible. As seen from Figure 3, complexation does not significantly affect the conformation of the macrocycles, as in the case of **C8HA**. The closest distances between S atoms of the macrocycles and carbon atoms of C60 are of 3.38 Å for **C8HA**, 3.39 Å for **C8MD**, and 3.44 Å for **C12HA**. In the case of methyl-substituted macrocycle **C12M**, the corresponding distances for **C12MC** and **C12MD** are 3.42 and 3.47 Å, close to that found for **C12HA** aggregate. Larger distance found for **C12MD** reflects steric hindrances caused by methyl groups for **D** complex. Therefore, both **C8** and **C12** are able to form inclusion complexes. Cyclooligothiophenes and C60 are also able to form complexes by the interaction of the π cloud of the macrocycle rim and the π system of C60 (**B**, **E**, and **F**). Actually, this type of complex is the most stable for **C12** according to experimental data.[13] Shortest C60−S distances in complexes of **C12H** and their linear analogue **L12** are very similar ranging from 3.41 to 3.44 Å. In the case of methyl-substituted macrocycles, these distances are slightly longer because of steric effects of methyl groups. This effect is the most notorious for **C12MF** complex because of the proximity of methyl groups and C60 (3.70 Å). For other complexes formed by **C12M**, these distances vary from 3.47 to 3.49 Å.

Binding Energies. Table 1 shows calculated binding energies in different complexes. As seen from the Table, the BSSE

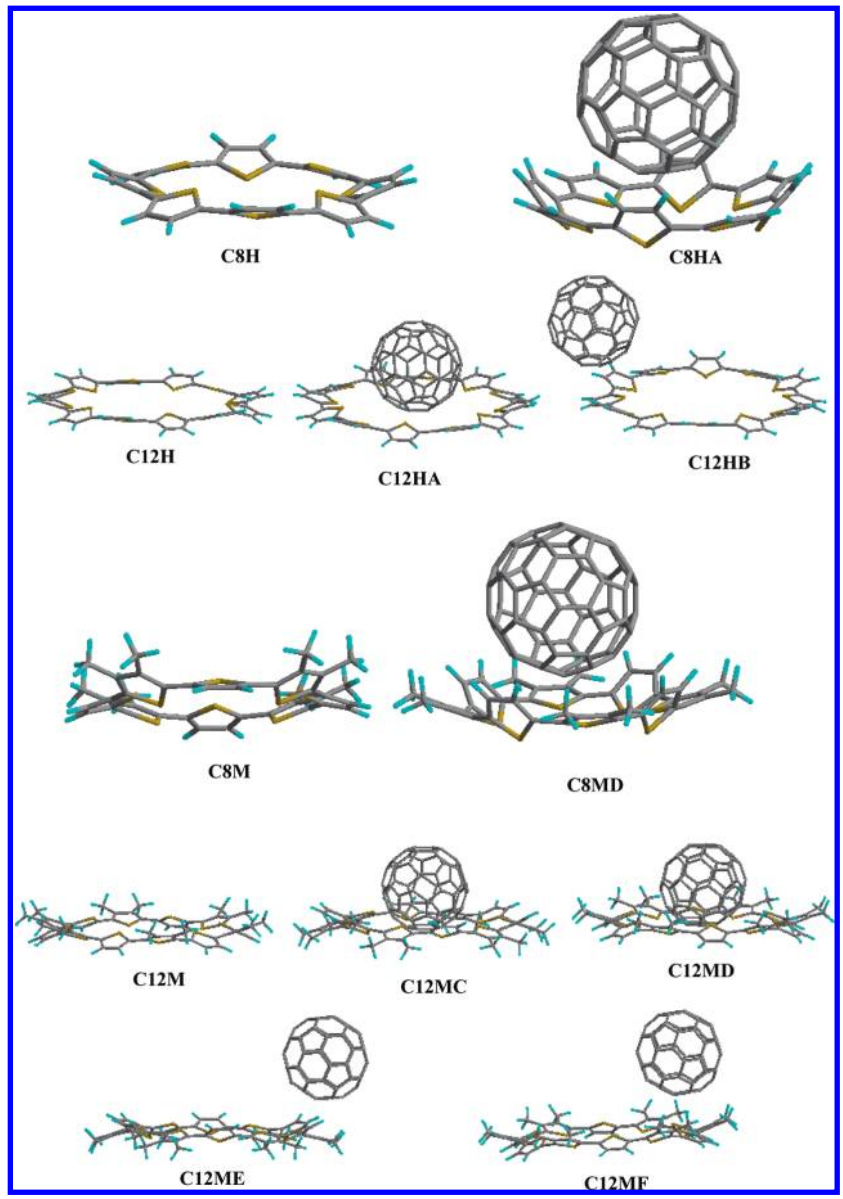

Figure 3. M05-2X/6-31G(d) optimized geometry of studied complexes. C60−cyclooligothiophene complexes are denoted as **CnXY**, where **n** is the number of thiophene units in cyclooligothiophene fragment, **X = H** for unsubstituted cyclooligothiophenes and **X = M** for methyl substituted analogues, and **Y** is the type of complex according to Figure 1.

represents a very important correction to the binding energy for certain type of complexes. Therefore, for the complexes formed by **C8H** or **C8M** macrocycles, the counterpoise correction represents more than a half of their binding energy because the geometry of **C8HA** and **C8MD** complexes favors large BSSE. For the complexes formed by linear oligothiophenes, BSSE is less important, and their relative stabilities are similar for BSSE-corrected and uncorrected energies.

The importance of taking into account BSSE for C60−cyclooligothiophene complexes can be illustrated by inspecting the relative stabilities of **C12MC** and **C12ME** complexes. According to experimental data,[13] **C12ME** is more stable compared with **C12MC**; nonetheless, uncorrected binding energies predict **C12MC** to be more stable compared with **C12ME** (Table 1). BSSE-corrected binding energies predict **C12ME** to be more stable in accordance with the experiment. As seen from the Table 1, BSSE is most important for **A** and **C** complexes. The binding energy of the complexes depends on two important factors: steric and electronic. As seen from the Table 1, the most stable complexes are **C8HA** and **C8MD** because of close matching between macromolecular cavity adopting conic shape and C60. The stability of "inclusion" complexes decreases from **C8** to **C12** because of the increasing mismatch between the size of the molecular cavity and C60. For **C12H** and **C12M** macrocycles, the "inclusion" complexes and those formed between C60 and a macrocycle rim have comparable binding energies (Table 1). The binding energies of **C12ME** and **C12MF** are higher compared with that of **C12HB**. This difference is due to the fact that **C12M** is a slightly better donor compared with **C12H**. Thus, HOMO level energies estimated as vertical ionization potentials (Table 3) are of 6.51 and 6.56 eV, respectively. Another factor is the macrocycle flexibility.

In fact, substituted macrocycles are more flexible compared with unsubstituted ones. The mechanism of this phenomenon is related to the fact that unsubstituted macrocycle possesses better conjugation than the substituted macrocycle, and any conformational change implies a decrease in conjugation, and consequently, the dihedral angles in **C12H** are of 31.9°, whereas in **C12M**, they are of 41.8°. Therefore, the loss of stabilization

TABLE 1: M05-2X/6-311G//M05-2X/6-31G* Counterpoise-Corrected (E_1) and Uncorrected (E_2) Binding Energies in kilocalories per mole, Charges on C60 Fragment in S0 (q_g) and S1 (q_{ex}) States in Neutral and Charged Complexes, and Charge Difference on C60 Fragment in S1 and S0 States (Δq)**

complex	E_1	E_2	q_{ex}	q_g	Δq
C8HA	11.37	18.3	–1.04	–0.06	0.98
C12HA	8.14	12.55	–1.07	–0.09	0.98
C12HB	6.49	9.21	–0.91	–0.02	0.89
LC8	8.10	10.99	–0.97	–0.03	0.94
LC12	7.56	10.12	–0.99	–0.03	0.96
C8MD	11.28	17.66	–1.04	–0.06	0.98
C12ME	7.79	10.67	–0.92	–0.03	0.89
C12MF	7.44	10.43	–0.89	–0.03	0.86
C12MC	5.27	12.72	–1.09	–0.1	0.99
C12MD	7.88	12.16	–1.08	–0.09	0.99
C8HA+	19.91	27.5		–0.03	
C8HA–	10.82	18.41		–0.97	
C8MD+	15.76	22.85		–0.03	
C8MD–	8.53	15.74		–0.97	
LC8+	6.64	9.21		0.02	
LC8–	8.06	10.95		–0.99	
C12HA+	8.61	12.97		–0.07	
C12HA–	5.03	10.17		–1.00	
C12HB+	6.26	8.93		–0.01	
C12HB–	6.48	9.16		–0.99	
LC12+	6.64	9.18		0.00	
LC12–	8.65	11.54		–0.99	
C12MD+	9.03	13.31		–0.07	
C12MD–	3.05	8.09		–1.00	
C12ME+	8.33	11.33		0.01	
C12ME–	7.85	10.72		–0.99	

TABLE 2: S0 → S1 Transition Energies (E_g, electronvolts) in Cyclooligothiophenes and C60−Cyclooligothiophene Complexes Estimated at TD-M05-2X/6-311G//M05-2X/6-31G* and TD-CAM-B3LYP/6-311G**//M05-2X/6-31G* Level of Theory**

molecule	E_g [a]	E_g [b]
C8HA	2.09	2.31
C12HA	2.31	2.58
C12HB	2.27	2.46
LC8	2.31	2.51
LC12	2.29	2.50
C8MD	2.03	2.26
C12ME	2.27	2.46
C12MF	2.37	2.53
C12MC	2.49	2.76
C12MD	2.48	2.55
C8H	3.16	3.14
C12H	2.89	2.87
C8M	3.26	3.24
C12M	3.25 (3.17)[c]	3.22
L8	2.76	2.73
L12	2.61	2.59

[a] M05-2X. [b] CAM-B3LYP. [c] Ref 24.

energy due to conformational changes is greater for unsubstituted macrocycles. This assumption is supported by calculations, and thus calculated rotational barriers for models I and II (Figure 4) are of 1.3 and 0.5 kcal/mol, explaining greater flexibility of methyl-substituted macrocycles and resulting in higher binding energies compared with those of unsubstituted macrocycles.

As seen from the Table 1, the BSSE-corrected binding energies of C60−cyclooligophenes complexes do not exceed 12 kcal/mol. BSSE-corrected binding energies of **C8H** dimer previously studied[12] and recalculated at the M05-2X/6-311(d,p)//M05-2X/6-31G(d) level to make possible comparison is of 24.5

TABLE 3: Vertical (v) and Adiabatic (a) Ionization Potential (IP), Electron Affinity (EA), and Relaxation Energies (λ_+, λ_-) Estimated at the M05-2X/6-311//M05-2X/6-31G* Level of Theory in electronvolts**

molecule	IP_v	IP_a	λ_+ [a]	EA_v	EA_a	λ_- [b]
C8H	6.89	6.64	0.25			
C12H	6.56	6.29	0.27			
L8	6.51	6.32	0.19			
L12	6.44	6.29	0.15			
C8M	6.64	6.44	0.20			
C12M	6.51	6.36	0.15			
C60				2.60	2.66	0.06
C8HA	6.65	6.36	0.29	2.50	2.64	0.06
C8MD	6.48	6.24	0.24	2.46	2.54	0.08
LC8	6.66	6.39	0.27	2.53	2.66	0.13
C12HA	6.51	6.27	0.24	2.47		
C12HB	6.54	6.30	0.24	2.56	2.66	0.10
LC12	6.55	6.34	0.21	2.56		
C12MD	6.53	6.31	0.22			
C12ME	6.53	6.34	0.19	2.56	2.66	0.10

[a] $\lambda_+ = IP_v - IP_a$. [b] $\lambda_- = EA_a - EA_v$.

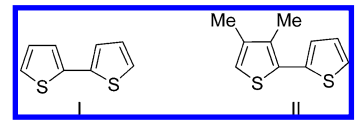

Figure 4. Model structures.

kcal/mol. Therefore, cyclooligophene−C60 complexes, at least those formed by **C8H**, are intrinsically unstable with respect to their dissociation to form two separate phases, C60 and cyclooligothiophene. C60−cyclooligothiophene interactions will only be observed at the interfaces. This observation is important in terms of photovoltaic device fabrication because it has been demonstrated that pure CT complexes show poor conversion efficiency,[1b] and molecular bulk heterojunction seems to be the best approach for organic solar cells.[23]

Excited State Properties. Table 2 shows S0 → S1 excitation energies for oligocyclothiophenes, their linear analogues, and the corresponding complexes with C60. As seen, the TD-M05-2x/6-311**//M05-2x/6-31G* model reproduces the experimental S0 → S1 energy with an error of only 0.07 eV for **C12M** macrocycle.[24] The comparison of TD-M05-2X and TD-CAM-B3LYP models for the calculation of excitation energies shows that whereas for the donor fragments both functionals deliver very similar results S0 → S1 energy for CT complexes is 0.19 to 0.27 eV higher for the CAM-B3LYP model, especially designed for the treatment of CT excited states,[25] demonstrating that the TD-M05-2x model produce very reasonably results for CT excited states. For **A**, **C**, and **D** "inclusion" complexes; the most important contribution for the S0 → S1 transition is HOMO → LUMO excitation (Table 2), whereas for the complexes formed at the macrocycle rim, there are a number of excitations involved in the S0 → S1 transition for C60−cyclooligothiophene complexes. To better visualize the nature of the electron excitations in CT complexes, natural transition orbitals were used.[26] Figure 5 depicts the dominant natural transition orbital pairs for S0 → S1 transitions in selected CT complexes. In all cases, the electron transfer from donor fragment to acceptor fragment (C60) occurs. It is noteworthy that in the case of **B**, **E**, and **F** complexes, where C60 interacts with the macrocycle rim, the electron transfer occurs mostly from the macrocycle part close to C60 (Figure 5). To monitor the change of the electron density on excitation, we also calculated the Mulliken charges in S0 and S1 states.

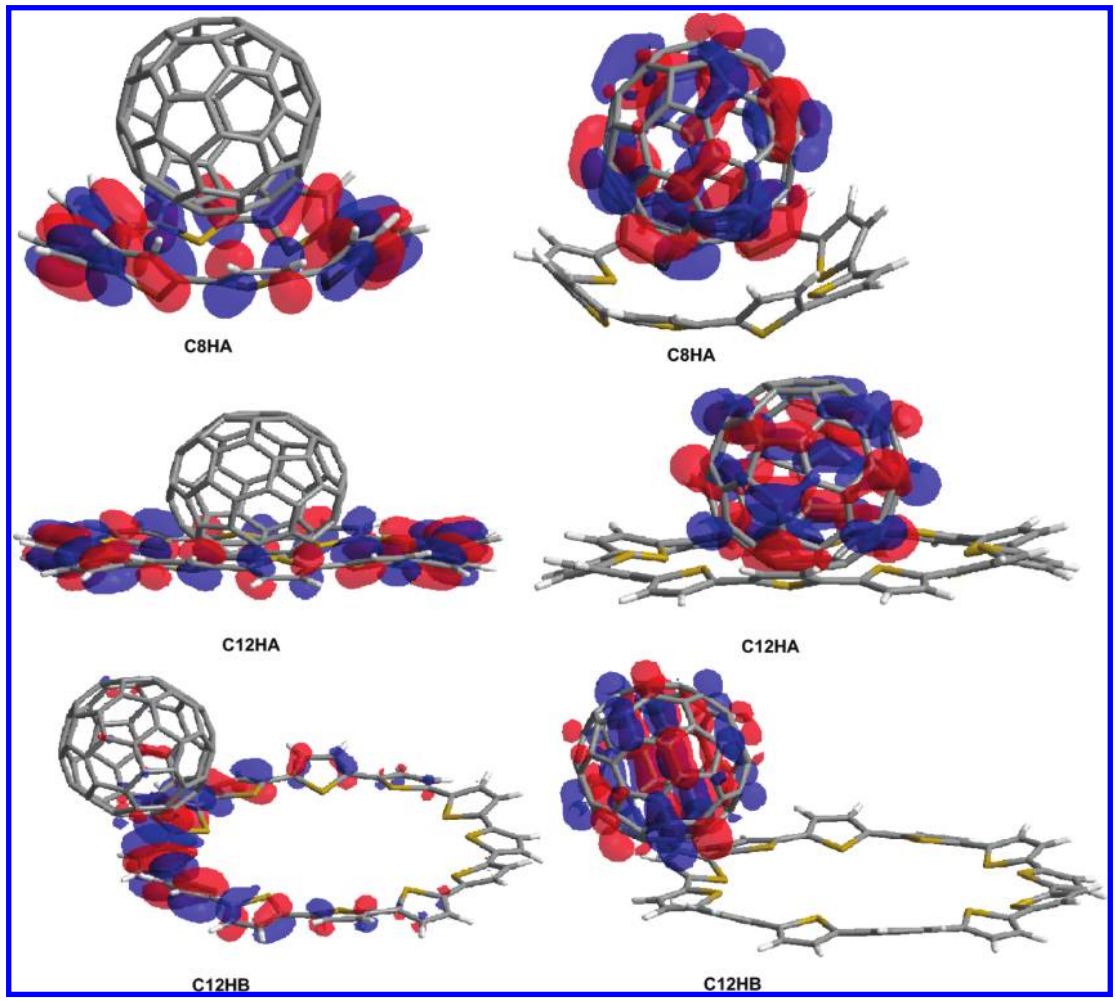

Figure 5. Dominant natural transition orbital pairs for S0 → S1 transitions in selected CT complexes. The "hole" is on the left, and the "particle" is on the right. The associated eigenvalues are 0.99, 0.98, and 0.99 for **C8HA**, **C12HA**, and **C12HB**, respectively.

As seen (Table 1), the CT in the ground state of the complexes is minimal, not exceeding 0.1 electron for **C12MC**. Complexes of **A**, **M**, and **C** types ("inclusion" complexes) show stronger CT in the ground state compared with **B**, **F**, and **E** types of complexes because of better overlapping between orbitals of the donor and the acceptor fragments in the former. The CT in the ground state of **LC8** and **LC12** complexes are similar to those formed between C60 and the macrocycle rim because of the similarity in the interaction pattern between donor and acceptor moieties. As seen from the Table 1, the excitation of the complexes results in almost complete electron transfer from donor fragment to C60 moiety. Therefore, for **C12MC** and **C12MD** complexes, the CT on excitation reaches 0.99 electron. Similarly to the ground state, the CT in the excited state is favored for **A**-, **M**-, and **C**-type complexes. The difference, however, between different types of complexes is minimal.

The energy of S0 → S1 transitions in cyclooligothiophene−C60 complexes varies from 2.03 eV for **C8MD** to 2.49 eV for **C12MC** (Table 2). S0 → S1 transition energies demonstrate certain correlation with the binding energies of the complexes (R^2 = 0.7). This phenomenon resembles well-established correlation between HOMO−LUMO energy differences of a donor and an acceptor, respectively, and stabilization energy of donor−acceptor complexes[27] because the S0 → S1 transition in studied complexes has a significant contribution from HOMO → LUMO excitation.

Cation and Anion Radicals. Table 1 presents binding energies of charged CT complexes. Electron detachment and electron attachment change the binding energies of CT complexes. Therefore, in all cases, both reduction and oxidation decrease the binding in all complexes except for **C8HA** and **C8MD**, where the oxidation leads to a significant increase in binding energies, whereas the reduction increases the binding energies only moderately. The reduction of binding energies in CT complexes on oxidation and reduction is in line with our previous work.[12b] In the case of oxidation, positive charge is localized at the donor fragment, whereas in the case of the reduction, the negative charge is located at acceptor fragment. Both oxidation and reduction decrease donor−acceptor interaction in CT complexes. As seen from the Table 1 and Figure 6, similar effect takes place in studied complexes. Therefore, in anion radicals, all negative charge is concentrated on the C60 fragment, whereas in cation radicals, all positive charge is located on the donor fragment. The abnormal behavior of **C8HA** and **C8MD** complexes on oxidation and reduction can be rationalized as follows: the origin of interactions in CT complexes is not entirely donor−acceptor; there is a significant contribution from dispersion interactions as well, which is a very short-range one.

The strength of dispersion interactions is related to the polarizability of the involved species. Table 4 lists calculated isotropic polarizabilities of neutral and charged species involved in CT complex formation. As seen, cation radicals of oligothiophenes (both cyclic and linear) possess much higher polarizabilities compared with neutral species. Polarizability of C60 increases only slightly on one electron reduction. Therefore, for

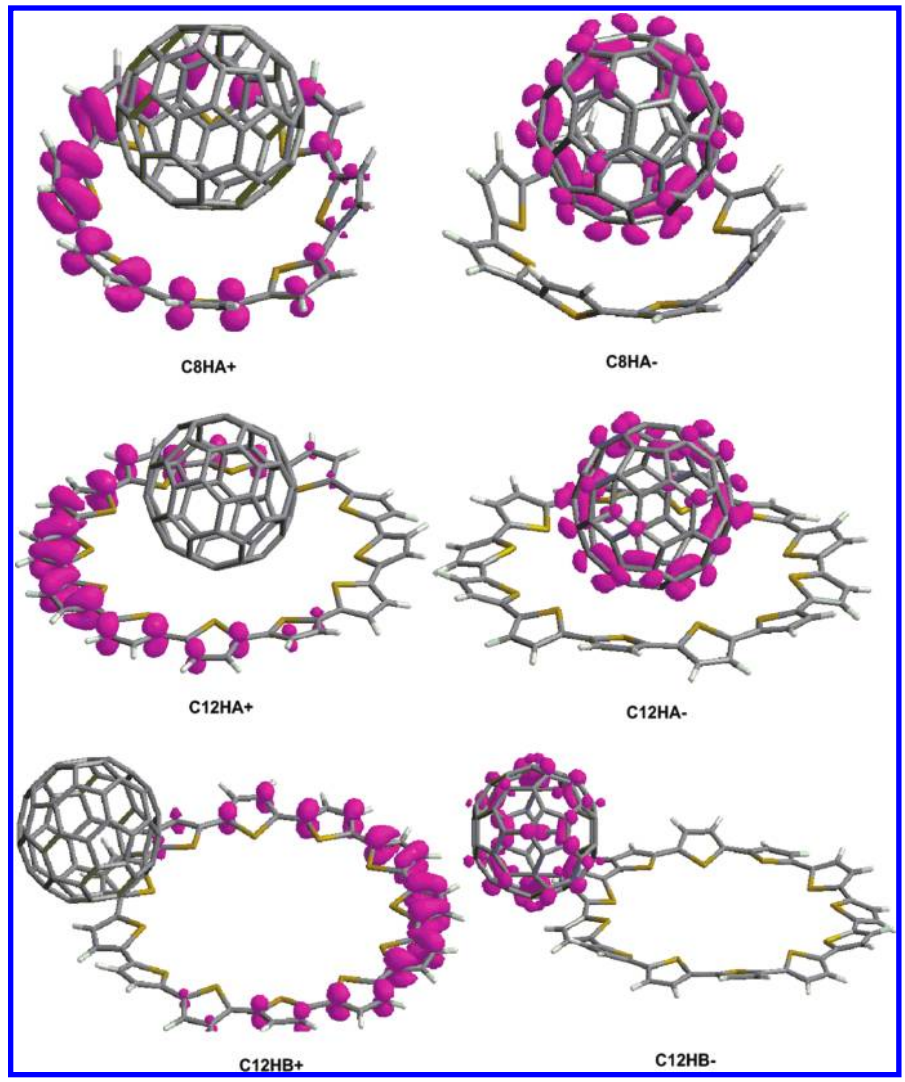

Figure 6. Spin density distribution in cation and anion radicals of selected complexes estimated at the M05-2X/6-311G(d,p)//M05-2X/6-31Gd level.

TABLE 4: Isotropic Static Polarizabilities of Oligothiophenes and C60 Estimated at M05-2X/6-311G// M05-2X/6-31* Level in au[3]**

molecule	neutral	cation	anion
L8	697.17	2523	
L12	1138	7816	
C8H	560.8	1543	
C12H	955.4	2552	
C8M	669.3	1777	
C12M	1076	2711	
C60	484.7		530.7

tight complexes such as **C8HA** and **C8MD**, oxidation leads to a notorious increase in dispersion interactions in CT complexes, overcompensating a decrease in donor−acceptor interactions. This effect is less notorious on the reduction because of the only moderate increase in the polarizability of C60 anion compared with neutral C60. Because dispersion is a short-range interaction, this effect can only be observed for tight **C8HA** and **C8MD** complexes. As seen from the Figure 6, the charge distribution is not symmetrical in cation radicals, which is related to large relaxation energies of cation radicals (Table 3) leading to the localization of a polaron cation.[28] It is noteworthy that in the case of **B**, **E**, and **F** complexes, the polaron cation is always located on the opposite side of the C60 molecule (Figure 6). The reduction of CT complexes changes very little the geometry of donor and acceptor components in CT complexes, which is reflected in low λ_- (Table 3) for anion radicals. The negative charge in anion radicals is mostly located in the C60 fragment, and its rigid structure impedes the deformation. There are notorious geometrical changes of the cyclooligothiophene component in cation radicals where aromatic structure is transformed to a quinoid structure in the area of localization of polaron cation. Therefore, the inter ring bond lengths shorten from 1.45 in neutral complexes to 1.41 Å in the area of localization of polaron cations in cation radicals.

Figure 7 shows a simplified energy diagrams modeling free charge photogeneration at the donor−acceptor interface. First, the excitation of a donor molecule leads to the exciton formation ($\mathbf{D} + \mathbf{A} \rightarrow \mathbf{D}^* + \mathbf{A}$ process). The exciton is modeled as a solvated S1 donor state. (See the Computational Details section.) There are two different ways to form free charges ($\mathbf{D}^+ + \mathbf{A}^-$) from exciton: the first one is direct exciton dissociation via "hot" CT states,[29] and the second one is the degradation of the exciton into S1 CT state (**DA**)*, which can dissociate to form free charge carriers ($\mathbf{D}^+ + \mathbf{A}^-$) or to relax into the ground-state CT complex (**DA**). As seen, the energy diagrams are different for different donors. Therefore, in the case of **C8HA** and **C8MD** complexes having high binding energies, the (**DA**)* state lies more than 1 eV below the energy level corresponding to separated charges impeding the free charge generation from the excited CT state,

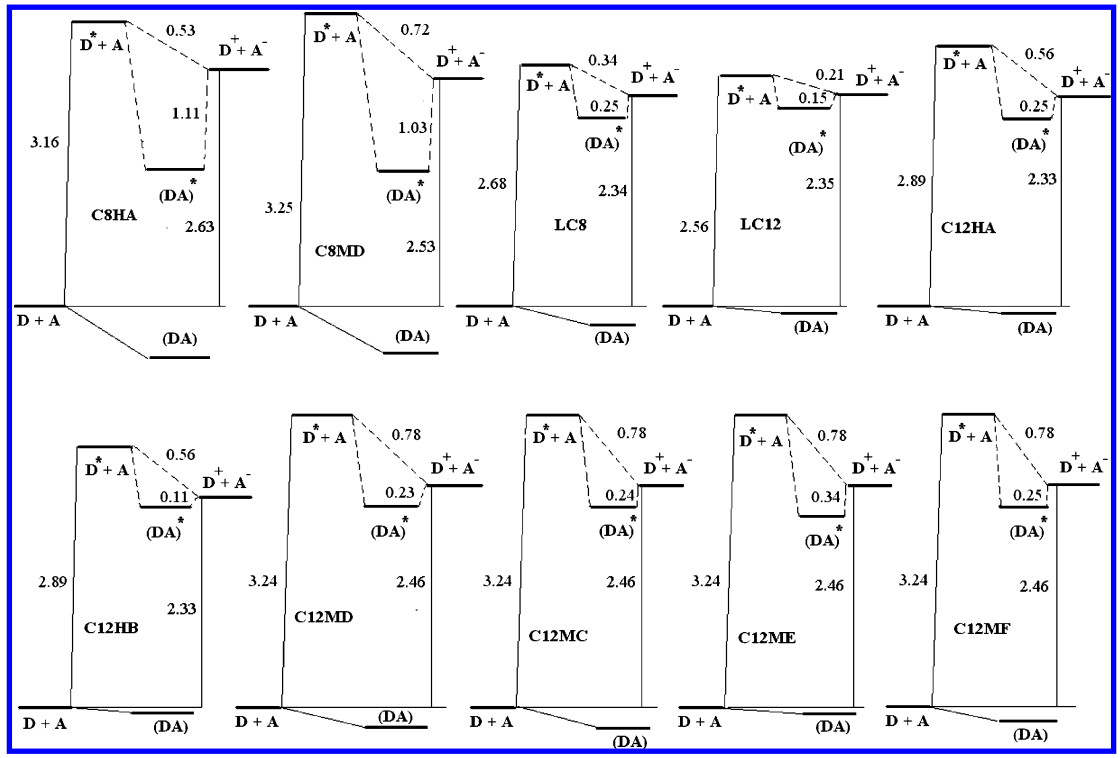

Figure 7. Electronic state diagram describing the photoinduced charge-carrier formation at C60−oligothiopene interface (in electronvolts). **D** + **A** is the sum of total electronic energies of oligothiophene (**D**) and C60 (**A**) molecules in their respective phases in S0 state. **D*** + **A** is the sum of total electronic energies of S1 state of **D** and S0 state of **A** in their respective phases. **(DA)*** is a total electronic energy of CT complex at the donor−acceptor interface in S1 state. **DA** is a total electronic energy of CT complex at the donor−acceptor interface in the S0 state. $\mathbf{D}^+ + \mathbf{A}^-$ is the sum of total electronic energies of free cation and anion radicals in their respective phases.

which is related to the additional energy required to separate closely positioned charges. In less stable CT complexes, the energy difference between (**DA**)* and $\mathbf{D}^+ + \mathbf{A}^-$ levels is far less, favoring the dissociation of (**DA**)* into the free charge carriers. This is especially notorious for the **LC12** complex, where the (**DA**)* → $\mathbf{D}^+ + \mathbf{A}^-$ energy difference is only 0.15 eV.

A sum of adiabatic ionization potential of a donor and electron affinity of an acceptor defines the upper limit for the open-circuit voltage of the solar cell, which represents a difference between **D** + **A** and $\mathbf{D}^+ + \mathbf{A}^-$ energy levels in Figure 7. The largest difference is for **C8HA** (2.63 eV), whereas the lowest one is for **LC12** (2.35 eV). However, the best relation between the S0 → S1 excitation energy of a donor and upper limit of the open-circuit voltage is for **LC8** and **LC12** (Figure 7). Because **L8** and **L12** are plane, S0 → S1 excitation energies are significantly lower compared with **C8** and **C12**, where dihedrals between thiophene fragments are significant. (See the Supporting Information.) IP's of linear and cyclic oligothiophenes are close (Table 3), decreasing the upper limit of the open-circuit voltage for complexes formed by cyclic oligothiophenes. This effect is even more notorious for methyl-substituted macrocycles because methyl substitution reduces the ionization potential while increasing the S0 → S1 excitation energy, promoting out-of-plane macrocycle conformation, as seen from the Table 2.

As seen from the Table 2, S0 → S1 energies for donor molecules are similar for TD-CAM-B3LYP and TD-M05-2X models (0.02 to 0.03 eV difference), whereas for CT complexes, the TD-CAM-B3LYP model gives S0 → S1 energies 0.07 to 0.27 eV higher compared with those of the TD-M05-2X model. This will cause a decrease in **D*** + **A** − **(DA)*** splitting (Figure 7) by 0.2 to 0.25 eV, which is less than the smallest **D*** + **A** − **(DA)*** splitting calculated for CT complexes. Thus, for **LC12**, where the splitting is of 0.36 eV when calculated with the TD-M05-2X model, TD-CAM-B3LYP decreases splitting to 0.13 eV. Therefore, both models predict similar photophysics for CT complexes.

Conclusions

Binding energies and geometry of CT C60−oligothiophene complexes depend on the architecture of the donor component. Moreover, BSSE should be taken into account for binding energy estimation. The strongest complexes are formed by **C8H** and **C8M** macrocycles. These macrocycles form only one type of complexes where C60 molecule is fitted into the macrocycle cavity, **C12H** and **C12M** are able to form a variety of CT complexes with C60, and their stability is similar to that formed by linear oligomers **L8** and **L12**. All complexes show little CT in the ground state. However, there is a complete electron transfer to C60 fragment in all complexes in the excited state. One electron oxidation or reduction of the complexes leads to the localization of positive or negative charge at the oligothiophene or C60 fragment, respectively. Relaxation energies were found to be significantly higher for cation radicals than for anion radicals.

Acknowledgment. This research was carried out with the support of grants IN100209 from PAPIIT and 49290 from CONACyT. We acknowledge the support of DGSCA and UNAM for using supercomputer KanBalam.

Supporting Information Available: Optimized Cartesian coordinates. This material is available free of charge via the Internet at http://pubs.acs.org.

References and Notes

(1) (a) Sariciftci, N. S.; Smilowitz, L.; Heeger, A. J.; Wudl, F. *Science* **1992**, *258*, 1474. (b) Tang, C. W. *Appl. Phys. Lett.* **1986**, *48*, 183.

(2) Bundgaard, E.; Krebs, F. C. *Sol. Energy Mater. Sol. Cells* **2007**, *91*, 954.

(3) Gunes, S.; Neugebauer, H.; Sariciftci, N. S. *Chem. Rev.* **2007**, *107*, 1324.

(4) (a) Koster, L. J. A.; Mihailetchi, V. D.; Bloom, P. W. *Appl. Phys. Lett.* **2006**, *88*, 93511. (b) Scharber, M. C.; Mühlbacher, D.; Koppe, M.; Denk, P.; Waldauf, C.; Heeger, A. J.; Brabec, C. J. *Adv. Mater.* **2006**, *18*, 789.

(5) Ma, W.; Yang, C.; Gong, X.; Lee, K.; Heeger, A. J. *Adv. Funct. Mater.* **2005**, *15*, 1617.

(6) Liang, Y.; Xu, Z.; Xia, J.; Tsai, S.-T.; Wu, Y.; Li, G.; Ray, C.; Yu, Y. *Adv. Mater.* **2010**, *22*, 1.

(7) (a) Krömer, J.; Rios-Carreras, I.; Fuhrmann, G.; Musch, C.; Wunderlin, M.; Debaerdemaeker, T.; Mena-Osteritz, E.; Bäuerle, P. *Angew. Chem.* **2000**, *112*, 3623. (b) Krömer, J.; Rios-Carreras, I.; Fuhrmann, G.; Musch, C.; Wunderlin, M.; Debaerdemaeker, T.; Mena-Osteritz, E.; Bäuerle, P. *Angew. Chem., Int. Ed.* **2000**, *39*, 3481. (c) Mena-Osteritz, E.; Bäuerle, P. *Adv. Mater.* **2001**, *13*, 243. (d) Fuhrmann, G.; Bäuerle, P. *Chem. Commun.* **2003**, 926. (e) Bäuerle, P.; Fischer, T.; Bidlingmeier, B.; Rabe, J. P.; Stabel, A. *Angew. Chem., Int. Ed.* **1995**, *34*, 303.

(8) (a) Nicolas, Y.; Blanchard, P.; Levillain, E.; Allain, M.; Mercier, N.; Roncali, J. *Org. Lett.* **2004**, *6*, 273. (b) Sun, X.; Liu, Y.; Chen, S.; Qiu, W.; Yu, G.; Ma, Y.; Qi, T.; Zhang, H.; Xu, X.; Zhu, D. *Adv. Funct. Mater.* **2006**, *16*, 917. (c) Kopidakis, N.; Mitchell, W. J.; van de Lagemaat, J.; Ginley, D. S.; Rumbles, G.; Shaheen, S. E.; Rance, W. L. *Appl. Phys. Lett.* **2006**, *89*, 103524.

(9) Bilge, A.; Zen, A.; Forster, M.; Li, H.; Galbrecht, F.; Nehls, B. S.; Farrell, T.; Neher, D.; Scherf, U. *J. Mater. Chem.* **2006**, *16*, 3177.

(10) (a) Ammann, M.; Rang, A.; Schalley, C. A.; Bäuerle, P. *Eur. J. Org. Chem.* **2006**, 1940. (b) Bäuerle, P.; Ammann, M.; Wilde, M.; Götz, G.; Mena- Osteritz, E.; Rang, A.; Schalley, C. A. *Angew. Chem., Int. Ed.* **2007**, *46*, 363.

(11) Jennings, W. B.; Farrell, B. M.; Malone, J. F. *Acc. Chem. Res.* **2001**, *34*, 885.

(12) (a) Flores, P.; Guadarrama, P.; Ramos, E.; Fomine, S. *J. Phys. Chem. A* **2008**, *112*, 3996. (b) Garcia, M.; Ramos, E.; Guadarrama, P.; Fomine, S. *J. Phys. Chem. A* **2009**, *113*, 2953.

(13) Mena-Osteritz, E.; Bäuerle, P. *Adv. Mater.* **2006**, *18*, 447.

(14) Liu, Z. T.; Lo, M. F.; Wang, H. B.; Ng, T. W.; Roy, V. A. L.; Lee, C. S.; Lee, S. T. *Appl. Phys. Lett.* **2009**, *95*, 093307.

(15) Zhao, Y.; Schultz, N. E.; Truhlar, D. G. *J. Chem. Theory Comput.* **2006**, *2*, 364.

(16) Bhattacharya, S. *Chem. Phys. Lett.* **2007**, *446*, 199.

(17) Fan, B.; Wang, P.; Wang, L.; Shi, G. *Sol. Energy Mater. Sol. Cells* **2006**, *90*, 3547.

(18) Frisch, M. J.; Trucks, G. W.; Schlegel, H. B.; Scuseria, G. E.; Robb, M. A.; Cheeseman, J. R.; Montgomery, J. A., Jr.; Vreven, T.; Kudin, K. N.; Burant, J. C.; Millam, J. M.; Iyengar, S. S.; Tomasi, J.; Barone, V.; Mennucci, B.; Cossi, M.; Scalmani, G.; Rega, N.; Petersson, G. A.; Nakatsuji, H.; Hada, M.; Ehara, M.; Toyota, K.; Fukuda, R.; Hasegawa, J.; Ishida, M.; Nakajima, T.; Honda, Y.; Kitao, O.; Nakai, H.; Klene, M.; Li, X.; Knox, J. E.; Hratchian, H. P.; Cross, J. B.; Bakken, V.; Adamo, C.; Jaramillo, J.; Gomperts, R.; Stratmann, R. E.; Yazyev, O.; Austin, A. J.; Cammi, R.; Pomelli, C.; Ochterski, J. W.; Ayala, P. Y.; Morokuma, K.; Voth, G. A.; Salvador, P.; Dannenberg, J. J.; Zakrzewski, V. G.; Dapprich, S.; Daniels, A. D.; Strain, M. C.; Farkas, O.; Malick, D. K.; Rabuck, A. D.; Raghavachari, K.; Foresman, J. B.; Ortiz, J. V.; Cui, Q.; Baboul, A. G.; Clifford, S.; Cioslowski, J.; Stefanov, B. B.; Liu, G.; Liashenko, A.; Piskorz, P.; Komaromi, I.; Martin, R. L.; Fox, D. J.; Keith, T.; Al.Laham, M. A.; Peng, C. Y.; Nanayakkara, A.; Challacombe, M.; Gill, P. M. W.; Johnson, B.; Chen, W.; Wong, M. W.; Gonzalez, C.; Pople, J. A. *Gaussian 09*, revision A.02; Gaussian, Inc.: Wallingford, CT, 2009.

(19) Runge, E.; Gross, E. K. U. *Phys. Rev. Lett.* **1984**, *52*, 997.

(20) Perdew, J. P.; Ruzsinsky, A.; Tao, J.; Staroverov, V. N.; Scuseria, G. E.; Csonka, G. I. *J. Chem. Phys.* **2005**, *123*, 06.

(21) San, S. E.; Yerli, Y.; Okutan, M.; Yilmaz, F.; Gunaydın, O.; Hamesc, Y. *Mater. Sci. Eng., B* **2007**, *138*, 284.

(22) Ruoff, R. S.; Tse, D. S.; Malhotra, R.; Lorents, D. C.; *J. Phys. Chem.* **1993**, *97*, 3379.

(23) Heremans, P.; Cheyns, D.; Rand, B. P. *Acc. Chem. Res.* **2009**, *42*, 1740.

(24) Bednarz, M.; Reinekera, P.; Mena-Osteritz, E.; Baüerle, P. *J. Lumin.* **2004**, *110*, 225.

(25) Yanai, T.; Tew, D.; Handy, N. *Chem. Phys. Lett.* **2004**, *393*, 51.

(26) Martin, R. L. *J. Chem. Phys.* **2003**, *118*, 4775.

(27) Kost, D.; Frailich, M. *THEOCHEM.* **1997**, *398*−*399*, 265.

(28) Fomine, S.; Guadarrama, P. *J. Phys. Chem. A* **2006**, *110*, 10098.

(29) Brédas, J.-L.; Norton, J. E.; Cornil, J.; Coropceany, V. *Acc. Chem. Res.* **2009**, *42*, 1691.

JP1007347